

# ROBUST OPTIMAL CONTROL OF NUCLEAR REACTORS AND POWER PLANTS

FISSION REACTORS

KEYWORDS: *robust control, optimal control, fault-accommodating control*

ROBERT M. EDWARDS, KWANG Y. LEE, and ASOK RAY  
*The Pennsylvania State University, 231 Sackett  
University Park, Pennsylvania 16802*

Received March 25, 1991

Accepted for Publication November 26, 1991

*The state feedback assisted control (SFAC) uses the concept of state feedback to modify the demand signal for an embedded classical output feedback controller to achieve an optimal control objective. It has been shown that the SFAC concept can improve the performance of primary coolant temperature control in a nuclear reactor.*

*How the embedded classical controller assists a state feedback controller in achieving improved performance and stability robustness, which play an important role in implementing optimal control algorithms for reactor control over a wide range of operations, including possible faulted conditions, is demonstrated. While the state feedback component improves system performance, the classical output feedback component enhances stability robustness.*

## I. INTRODUCTION

In Ref. 1, which describes the state feedback assisted control (SFAC) configuration, the emphasis is on system dynamic performance by application of the optimal control theory. This approach primarily provides transparency of control to facilitate implementation of optimal control techniques within the established structures of power plant operations. A major concern in implementing optimal nuclear power plant control is that the model used to formulate an optimal control law cannot exactly match the physical process dynamics. Robust control theory and design address this concern by explicitly considering the discrepancy between the model used in an optimal control law and the actual process. In robust control terminology,<sup>2</sup> the discrepancy between the actual process and its model is referred to as uncertainty and can arise from the following three major sources:

1. The plant model (on which the controller is based) may be linear, whereas the actual process is essentially nonlinear.
2. The plant model is made to be of lower order than the actual plant (e.g., a lumped parameter model of a distributed parameter process).
3. The model parameters may not be correct because of variations in normal plant operation, plant degradations, and faults.

A controller can be defined as robust if system dynamic performance and stability criteria are met while accounting for a specified range of uncertainties and disturbances.<sup>2</sup> On the other hand, the goal of a fault-accommodating controller is to make the control system tolerant of faults in one or more components. Therefore, the functionalities of robustness and fault accommodation are overlapping. A control system has a robust design when the effects of postulated uncertainties, modeling errors, and noise expected to be prevalent under normal operations are taken into account. These effects include *soft* failures, i.e., those having power spectra comparable to the postulated noise and uncertainties. In the event of *hard* failures, i.e., large disruption(s) caused by internal disturbances, externally induced disruptions, or failures of plant components and instrumentation, the control system may have to be reconfigured on-line using one of the viable pre-designed options.<sup>3</sup> The reconfigured control system must be stable, although its performance is likely to be degraded. Control system reconfiguration for nuclear reactors is a subject for future research.

This paper demonstrates the robustness of the SFAC configuration in the sense that SFAC can more effectively accommodate plant modeling errors and disturbances than can a conventional state feedback controller (i.e., one without an embedded classical control loop). This robustness is demonstrated by examining the sensitivity of the system's dominant eigenvalues to expected variations in plant parameters, nonlinear-

ities, and higher order dynamics. The dominant eigenvalues of a more robust system should be less sensitive to these uncertainties. Time domain simulation is also presented to confirm the desirable response due to the SFAC system's less sensitive dominant eigenvalues. The superior robustness of the SFAC configuration to uncertainties is also expected to result in better fault-accommodating characteristics.

This paper has seven sections. Section I is the introduction. Section II reviews the concept of SFAC and its application to reactor control where the plant model is assumed to be an exact representation of the actual process. Section III presents an optimal control law based on estimated states where the effects of modeling errors, uncertainties, and disturbances are taken into account. A general sensitivity analysis for an observer-based state feedback controller is presented in Sec. IV and applied to demonstrate the superior robustness of SFAC in Sec. V. Section VI further demonstrates the improved robustness with time domain simulation results. Section VII provides the summary and conclusions.

## II. REVIEW OF SFAC OPTIMAL REACTOR CONTROLLER DESIGN

Figure 1 presents the SFAC configuration for reactor power control. In the embedded classical control loop, reactor power is regulated solely by a conventional output feedback control law that simply multiplies its error signal (i.e., the modified setpoint  $n_m$  minus output  $n_r$ ) by a gain  $G_c$  to generate the com-

mand signal for control rod speed  $z_r$ . Reactivity due to control rod movement  $\delta\rho_r$  is symbolically represented as the control rod worth per unit length  $G_r$  times the integral of control rod speed. The plant responds to the control rod reactivity changes with a change in power  $n_r$  and internal reactivity feedback mechanisms. The state feedback control loop creates the modified demand signal  $n_m$  to achieve an optimal control performance objective. The algorithm for estimation of states (including the unmeasured internal states of the process) is based on a dynamic model of the physical process, the control input  $z_r$ , and plant output  $n_r$ . This state estimate  $\hat{x}$  has five components:

1. reactor power
2. precursor density
3. average reactor fuel temperature
4. average coolant temperature leaving the reactor
5. control rod reactivity.

The state feedback control is obtained as  $F_m \hat{x}$  where the gain matrix  $F_m = [f_{m1} \ f_{m2} \ f_{m3} \ f_{m4} \ f_{m5}]$ .

In contrast to the SFAC configuration, a conventional state feedback control (CSFC) configuration without an embedded classical controller directly manipulates the control rod speed, as shown in Fig. 2. Reference 1 introduces a formula for calculating state feedback gains for the SFAC configuration  $v_m$  and  $F_m$  from the CSFC gains  $v$  and  $F$  to account for the presence of the embedded controller with gain  $G_c$  as follows:

$$F_m = C + F/G_c$$

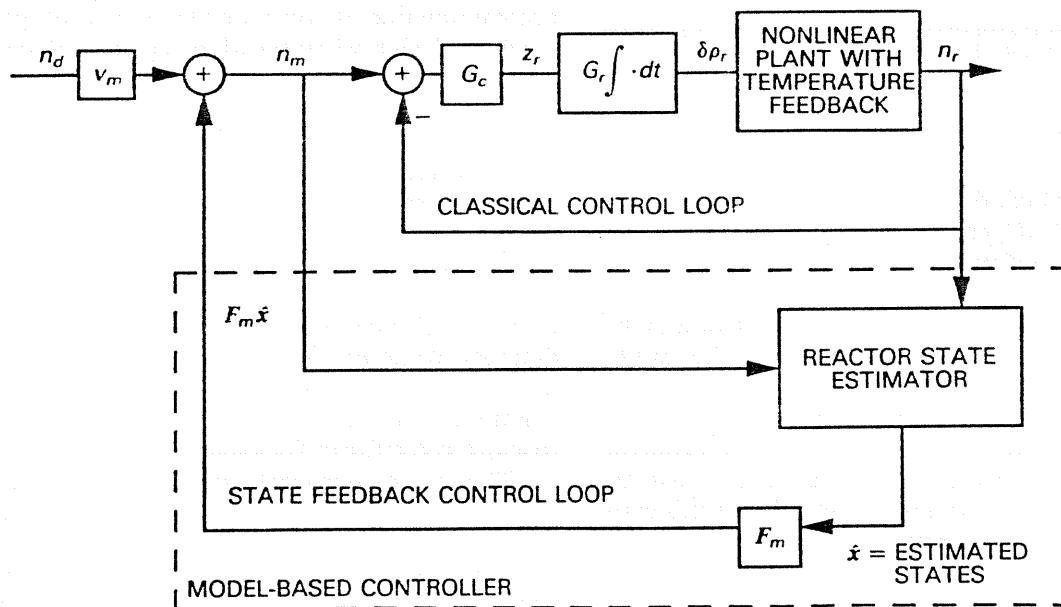


Fig. 1. The SFAC where the setpoint to an embedded classical controller is modified by state feedback to accomplish an optimal control objective.

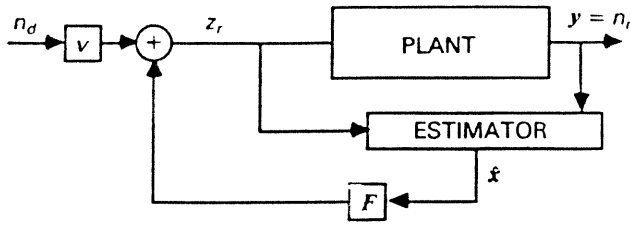


Fig. 2. CSFC where an optimal control objective is met by direct manipulation of the control variable.

and

$$v_m = v/G_c, \tag{1}$$

where the matrix **C** relates the output signal **y** to the state vector **x**,  $y = \mathbf{C}\mathbf{x}$ , in a state-space representation.

A nonlinear model using point kinetics with one-delayed neutron group and a two-temperature feedback mechanism<sup>1</sup> is the basis of a fifth-order model-based optimal reactor power controller for a pressurized water reactor (PWR). A state-space representation, based on a linearized version of the model, is

The symbol  $\delta$  indicates the deviation of a variable from an equilibrium value; e.g.,  $\delta n_r(t) = n_r(t) - n_{r0}$  with  $n_{r0} \equiv$  the nominal value of  $n_r$  at the equilibrium condition. The elements of the state, control, and output vectors are thus formed from the following process variables where

- $n_r \equiv n/n_0$  relative neutron density
- $n \equiv$  neutron density (per  $\text{cm}^3$ )
- $n_0 \equiv$  equilibrium neutron density at 100% power
- $c_r \equiv c/c_0$  relative precursor density
- $c \equiv$  delayed neutron precursor density (per  $\text{cm}^3$ )
- $c_0 \equiv$  equilibrium precursor density at 100% power
- $T_f \equiv$  average reactor fuel temperature ( $^\circ\text{C}$ )
- $T_l \equiv$  average coolant temperature leaving reactor ( $^\circ\text{C}$ )
- $\delta\rho_r \equiv$  change in control rod reactivity ( $\Delta k/k$ )
- $z_r \equiv$  control rod speed (fraction of core length/s).

The **A**, **B**, and **C** matrices in the state-space representation are

$$\mathbf{A} = \begin{bmatrix} -\beta/\Lambda & \beta/\Lambda & n_{r0}\alpha_f/\Lambda & n_{r0}\alpha_c/2\Lambda & n_{r0}/\Lambda \\ \lambda & -\lambda & 0 & 0 & 0 \\ f_f P_{0a}/\mu_f & 0 & -\Omega/\mu_f & \Omega/2\mu_f & 0 \\ (1-f_f)P_{0a}/\mu_c & 0 & \Omega/\mu_c & -(2M+\Omega)/2\mu_c & 0 \\ 0 & 0 & 0 & 0 & 0 \end{bmatrix},$$

$$\mathbf{B} = \begin{bmatrix} 0 \\ 0 \\ 0 \\ 0 \\ G_r \end{bmatrix},$$

and

$$\mathbf{C} = [1 \ 0 \ 0 \ 0 \ 0], \tag{4}$$

where

- $\beta \equiv$  fraction of fission neutrons that are delayed
- $\Lambda \equiv$  effective prompt neutron lifetime (s)
- $\lambda \equiv$  delayed neutron precursor radioactive decay constant ( $\text{s}^{-1}$ )
- $n_{r0} \equiv$  relative neutron density at an equilibrium point
- $\alpha_f \equiv$  fuel temperature reactivity coefficient ( $\Delta k/k \cdot ^\circ\text{C}^{-1}$ )

and

$$\dot{\mathbf{x}} = \mathbf{A}\mathbf{x} + \mathbf{B}\mathbf{u}$$

$$\mathbf{y} = \mathbf{C}\mathbf{x}, \tag{2}$$

where the state **x**, output **y**, and control **u** vectors are

$$\mathbf{x} = [\delta n_r \ \delta c_r \ \delta T_f \ \delta T_l \ \delta\rho_r]^T,$$

$$\mathbf{y} = [\delta n_r],$$

and

$$\mathbf{u} = [z_r]. \tag{3}$$

$\alpha_c \equiv$  coolant temperature reactivity coefficient ( $\Delta k/k \cdot ^\circ\text{C}^{-1}$ )

$P_{0a} \equiv$  design power level (MW)

$f_f \equiv$  fraction of reactor power deposited in fuel

$\mu_f \equiv$  heat capacity of the fuel (MW·s/°C)

$\Omega \equiv$  fuel-to-coolant heat transfer coefficient (MW/°C)

$\mu_c \equiv$  heat capacity of the coolant (MW·s/°C)

$M \equiv$  mass flow rate times heat capacity of the coolant (MW/°C)

$G_r \equiv$  reactivity worth of the rod ( $\Delta k/k$ ).

In Ref. 1, an optimal controller was designed on the basis of the foregoing model. The controller performance was then evaluated in the absence of any modeling errors and disturbances for a narrow power range (100 to 110% power). The equilibrium relative power level  $n_{r0}$  was set to 1.0. However, wide range variations in the parameter  $n_{r0}$  due to the nonlinear characteristic of a reactor as well as to other parameter variations is a major concern in evaluating and comparing the robustness characteristics of the SFAC and CSFC configurations. In this paper, we have used the middle of cycle full power plant parameters, given in Table I, to design a robust fifth-order model-based reactor power controller for a complete fuel cycle of a Three Mile Island (TMI)-type PWR (Ref. 4).

Optimal control gains for the CSFC configuration are calculated for the model parameters listed in Table I using the linear quadratic regulator approach<sup>5</sup> in order to minimize the following optimal control performance objective function:

$$J(z_r) = \int_0^\infty [0.01\delta T_f^2 + 0.1\delta T_c^2 + 3000z_r^2] dt, \quad (5)$$

subject to the state equation constraint given by Eq. (2). The weighting factors 0.01 and 0.1 on the reactor temperatures in Eq. (5) effectively yield an optimal controller to vary the reactor power, which is not penalized, while tightly controlling the reactor temperatures. Alternatively, if the reactor power state is assigned a non-zero penalty, then reactor temperature response would be more sluggish. Since instantaneous values of reactor temperatures determine the structural integrity of the reactor core more so than does the instantaneous value of reactor power, specifying control performance objectives on temperature states is more direct in achieving desirable system response. The resulting state feedback gain vector for achieving improved reactor temperature response is

$$F = [-0.0001431 \quad -0.1392 \quad -0.0002678 \quad +0.0004695 \quad -31.42] . \quad (6)$$

TABLE I

Parameters for Optimal Controller Design at the Middle of the Fuel Cycle of a TMI-Type PWR\*

$\beta$	= 0.006019
$\Lambda$	= 0.00002 s
$\alpha_f$	= -0.0000324 $\Delta k/k \cdot ^\circ\text{C}^{-1}$
$P_{0a}$	= 2500 MW
$\mu_f$	= 26.3 MW·s/°C
$\Omega$	= 6.6 MW/°C
$G_r$	= 0.01450 $\Delta k/k$
$\lambda$	= 0.150 s <sup>-1</sup>
$\alpha_c$	= -0.000213 $\Delta k/k \cdot ^\circ\text{C}^{-1}$
$f_f$	= 0.92
$\mu_c$	= 71.8 MW·s/°C
$M$	= 102.0 MW/°C

\*See Ref. 4.

Selection of the performance index  $J(\bullet)$  is critical for achieving a robust control design because it also has a direct bearing on the location of the closed-loop poles. Closed-loop poles for the nominal plant with a high damping ratio provide a stability margin to accommodate uncertainties. To consider the impact of uncertainties on the stability of an idealized full state feedback system, the sensitivity of the closed-loop poles, eigenvalues of the state feedback matrix  $A + BF$ , should be examined. An idealized full state feedback system, as referred to here, is a system where all the states can be perfectly measured and used directly in a feedback control law. In an idealized full state feedback system, an estimator is not needed, and the concerns about introducing an uncertain estimator are temporarily ignored. As the optimal regulator gain vector  $F$  is held fixed at that calculated value for the nominal plant parameters of a state-space model  $A$  and  $B$  matrices, the eigenvalues of the closed-loop system then vary as the parameters of the  $A$  and  $B$  matrices are varied (i.e., uncertainties are introduced). The parameter  $n_{r0}$  of Eq. (4) is due to the linearization of the nonlinear model about an equilibrium power level.<sup>1</sup> Variation of this parameter from the design value ( $n_{r0} = 1.0$ ) thus permits examination of the major nonlinear effect of reactor kinetics as a parameter uncertainty in the linearized state-space representation of a robust controller design. The parameter  $n_{r0}$  is the variable or nonlinear gain of a reactor transfer function.<sup>6</sup> While all the parameters of the model actually change with the reactor operating condition, they do not vary in direct proportion to the reactor power level.

Variations in  $n_{r0}$  receive initial priority in establishing robustness of a reactor controller. The eigenvalues of the idealized full-state feedback system  $\mathbf{A}(n_{r0}) + \mathbf{B}\mathbf{F}$  as the parameter  $n_{r0}$  is varied from 1.2 to 0.1 (120 to 10% power) is shown in Fig. 3. Figure 3 is similar to a root locus  $s$ -plane presentation. The complex conjugate pair of dominant eigenvalues (the characteristic equation roots) approach the real axis as power is reduced below 20%. These eigenvalues merge at a point on the real axis and then proceed in opposite directions along the real axis as power is reduced further. In Fig. 3 and the remaining figures (which are essentially similar), many other less sensitive eigenvalues also trace out loci of points in the complex plane. Although the eigenvalue with the smallest real part ultimately dominates the time domain response, we consider the eigenvalue that is most sensitive to parameter variations as the dominant one from the standpoints of performance and stability robustness.

The dominant eigenvalue location for the nominal plant (100% power  $\equiv n_{r0} = 1.0$ ) has a good damping ratio greater than 0.9. As power level is increased from 100 to 120%, the magnitude (speed of response) and damping ratio of the dominant eigenvalue increase slightly. As power is reduced to  $\sim 60\%$  power, the magnitude and damping ratio decrease slightly. Going from 60 to 10% power, the magnitude decreases further as the system moves to an overdamped condition. Although the optimal control design is strictly optimal with respect to Eq. (5) only at the 100% power condi-

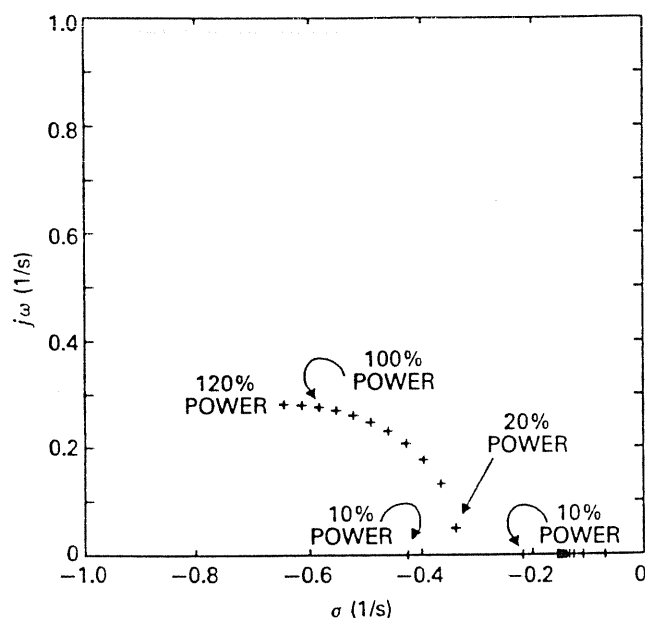


Fig. 3. Dominant eigenvalue sensitivity of an idealized fifth-order optimal control law due to the nonlinear characteristic of reactor power level in the range from 120 to 10% power at 10% intervals.

tion, the sensitivity characteristic of the dominant eigenvalue due to the major nonlinearity of the reactor is acceptable for this particular optimal control design from a stability standpoint.

### III. AN OPTIMAL OBSERVER APPROACH

Examination of the sensitivity of the closed-loop system's dominant eigenvalue for the idealized full state feedback case is of course only a first-level evaluation of a robust design. If the sensitivity at that level does not look favorable, there is no point in considering the less than ideal case of implementation with an uncertainty-prone model-based estimate of plant states. Good optimal controller performance and robustness in the idealized case should be obtained before designing an optimal observer for use in the controller.

Figure 4 shows the structure of a linear Luenberger Observer<sup>7</sup> for estimating unmeasured plant states. The nominal plant model  $\{\mathbf{A}_o, \mathbf{B}_o, \mathbf{C}_o\}$ , used in the design of an optimal control law  $\mathbf{F}$ , is the basis of a linear simulation operated in parallel with the plant to estimate the plant states. The design of robust optimal control takes into account uncertainties between the actual plant  $\{\mathbf{A}, \mathbf{B}, \mathbf{C}\}$  and the nominal model  $\{\mathbf{A}_o, \mathbf{B}_o, \mathbf{C}_o\}$  that is used for constructing the observer.

For the idealized case where the plant exactly matches the nominal plant, the observer gains can be made arbitrarily large in order to generate state estimates to rapidly track the plant states. If a stochastic component in the input, plant, or output measurements is considered, then the Kalman Filter<sup>8</sup> procedure provides appropriate estimator gains and structure to minimize the mean-square error between plant and estimated states. If external disturbances at the plant input and output are additionally considered, then the Linear Quadratic Gaussian/Loop Transfer Recovery (LQG/LTR) robust control design procedure<sup>9</sup> modifies the Kalman Filter procedure to accomplish a robust control design. The LQG/LTR control design indirectly accommodates some uncertainties but suggests the use of large observer gains.<sup>4,10,11</sup> The rationale for the robustness characteristics of the LQG/LTR procedure is that external disturbances at the plant input qualitatively mimic the effect of uncertainties. In an optimal observer approach, the possibility of external disturbances was ignored, and a low gain observer with good robustness to uncertainties was experimentally determined and later shown to minimize an optimal observer quadratic performance objective.<sup>4</sup> The robust optimal observer gain  $\mathbf{L}$  is computed from an optimal regulator control law  $\mathbf{F}_d$  for the dual system  $\{\mathbf{A}_o^T, \mathbf{C}_o^T\}$  with weighting matrices  $\{\mathbf{Q}_o, \mathbf{R}_o\}$ ; i.e.,  $\mathbf{L} = -\mathbf{F}_d^T$ . The dynamics of the dual system is related to the dynamics of the error between actual plant states and estimated plant states in a Luenberger Observer. The weighting matrix  $\mathbf{Q}_o$  is thus chosen to penalize state

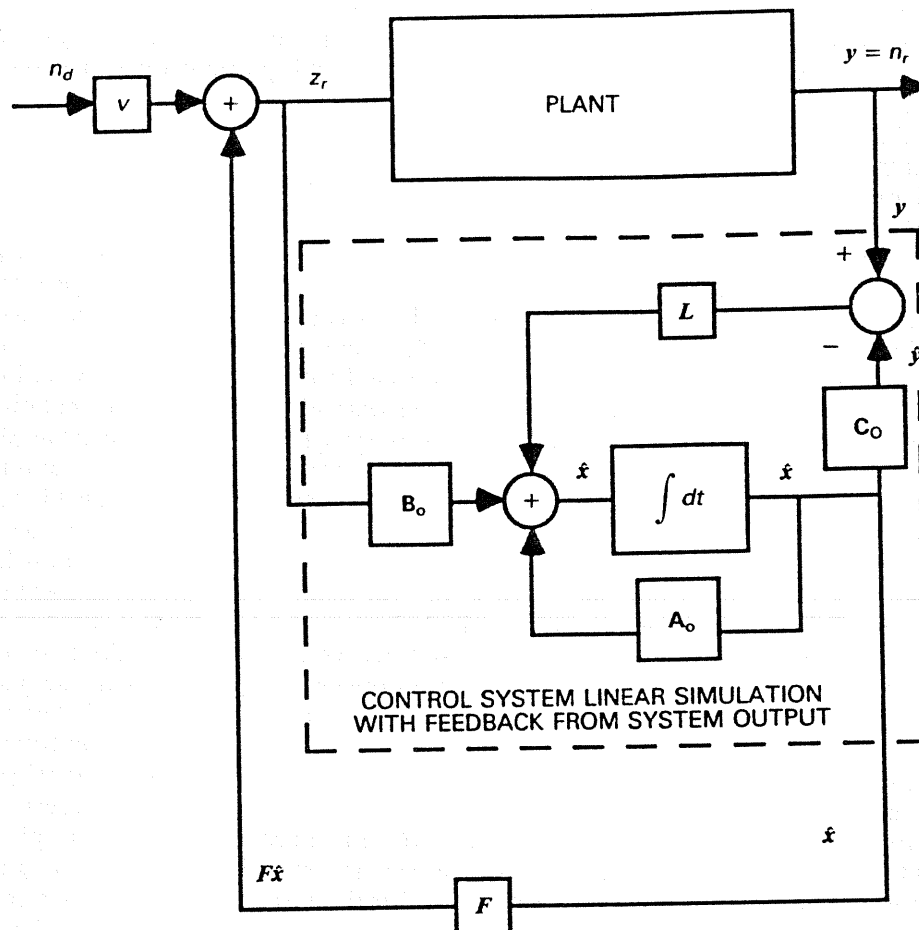


Fig. 4. CSFC configuration with a linear Luenberger Observer for estimating plant states.

estimation errors of importance to accomplish the specific optimal control law [Eq. (5)]. This importance is indicated by the relative magnitude of the individual elements of the state feedback gain vector [Eq. (6)]. The most important state estimates to accomplish the optimal control performance objective [Eq. (5)] are (a) precursor density, state 2 with feedback gain  $f_2 = -0.1392$ , and (b) control rod reactivity, state 5 with feedback gain  $f_5 = -31.42$ . Correct estimates of the other states are not as important as correct estimates for these states; therefore, the diagonal elements of  $\mathbf{Q}_o$  are chosen as the square of the corresponding state feedback gain vector element; i.e.,  $q_{ii} = f_i^2$ . (The off-diagonal elements of  $\mathbf{Q}_o$  are chosen as zero.)

For an optimal observer design,  $\mathbf{R}_o$  is interpreted as a penalty on the error between plant output  $y$  and estimated plant output  $\hat{y}$ , an input to the observer. For the single input/single output reactor control problem considered here, the  $\mathbf{R}_o$  matrix is simply a scalar  $r_o$ . The specification of the  $r_o$  penalty on the plant output error can be made very small to permit the plant output error to deviate more from zero while holding the state-estimate errors close to zero. When this is done, the resulting observer gains are identical to the LQG/

LTR procedure results.<sup>4</sup> Alternatively, a robust low gain optimal observer is obtained by making  $r_o$  large to permit the state estimate errors to deviate more from zero while holding the plant output error close to zero.<sup>4</sup> The rationale for this approach is that the state estimate errors must remain reasonable when the plant output error is forced toward zero because the plant output error is actually a function of the uncertainties that combine to produce the estimate errors in the first place. Selecting  $r_o = 5\,000\,000$  yields the following low observer gains whose robustness characteristics are demonstrated in comparing the SFAC and CSFC configurations in Sec. IV:

$$L = [2.007 \quad 0.1325 \quad 72.86 \quad 3.459 \quad 0.01405]^T. \quad (7)$$

#### IV. SENSITIVITY ANALYSIS OF AN OBSERVER-BASED OPTIMAL CONTROL

For the realistic implementation of an optimal control law using an on-line real-time model-based estimate of plant states, the closed-loop system's dynamic characteristics become more sensitive to uncertainties. Regardless of whatever approximate method is used to

suggest observer gains, the sensitivity of the eigenvalues of a model-based Luenberger Observer state feedback system can be precisely examined using an augmented state vector that includes both plant and observer as follows:

$$x_a = [x^T | \hat{x}^T]^T = [\delta n_r \quad \delta c_r \quad \delta T_f \quad \delta T_l \quad \delta \rho_r \quad \delta \hat{n}_r \quad \delta \hat{c}_r \quad \delta \hat{T}_f \quad \delta \hat{T}_l \quad \delta \hat{\rho}_r]^T, \quad (8)$$

where the caret symbol indicates an estimate of the corresponding state. For the CSFC configuration (Fig. 4), the augmented state-space representation matrices are

$$A_a = \left[ \begin{array}{c|c} \mathbf{A} & 0 \\ \hline \mathbf{LC} & \mathbf{A}_o - \mathbf{LC}_o \end{array} \right],$$

$$B_a = \left[ \begin{array}{c} \mathbf{B} \\ \mathbf{B}_o \end{array} \right],$$

and

$$F_a = \left[ \begin{array}{c} 0 \\ \mathbf{F} \end{array} \right]. \quad (9)$$

The closed-loop poles that characterize the combined model-based observer feedback system are the eigenvalues of the matrix  $A_a + B_a F_a$ . Note that the combined model only incorporates feedback of the estimated plant states in the augmented state feedback gain vector  $F_a$ . For the SFAC configuration (Fig. 1), the augmented state-space representation matrices are different because of the embedded classical controller with gain  $G_c$  as follows:

$$A_s = \left[ \begin{array}{c|c} \mathbf{A} - G_c \mathbf{B} \mathbf{C} & 0 \\ \hline L_m \mathbf{C} & \mathbf{A}_o - G_c \mathbf{B} \mathbf{C} - L_m \mathbf{C}_o \end{array} \right],$$

$$B_s = G_c \left[ \begin{array}{c} \mathbf{B} \\ \mathbf{B}_o \end{array} \right],$$

and

$$F_s = \left[ \begin{array}{c} 0 \\ \mathbf{F}_m \end{array} \right]. \quad (10)$$

where  $L_m$  is a modified observer gain vector for a plant model with an embedded classical controller to accomplish the same observer design objective as a CSFC observer design  $L$ .

The important thing to note between the CSFC [Eq. (9)] and the SFAC [Eq. (10)] augmented matrices is that the SFAC matrices have an additional parameter, the embedded classical controller gain  $G_c$ . Also recall that the SFAC state feedback gains  $F_m$  are adjusted according to Eq. (1) to account for the presence of the embedded classical controller. When the plant and observer are the same ( $\mathbf{A} = \mathbf{A}_o$ ,  $\mathbf{B} = \mathbf{B}_o$ , and  $\mathbf{C} = \mathbf{C}_o$ ), then the CSFC and SFAC configurations are equivalent and demonstrate the same robustness characteristics to uncertainties; the embedded classical controller gain can be chosen arbitrarily as a nonzero value. When the plant and observer are different, as they will always be for any real world application, then

the SFAC configuration demonstrates improved robustness characteristics over a CSFC implementation for the same optimal control law and positive values of  $G_c$ . The SFAC and CSFC configurations demonstrate different robustness characteristics when uncertainty is introduced because of the manner in which the formula for  $F_m$  [Eq. (1)] was derived.<sup>1</sup> At a certain point in the block-diagram logic derivation of Eq. (1), an estimate of the plant output  $\hat{y}$  and plant output  $y$  were introduced as an approximate cancellation at the summer shown in Fig. 5. When the plant and observer are the same, this cancellation is exact, and the two configurations are equivalent. When the plant and observer are not the same, the plant output  $y$  and estimated output  $\hat{y}$  will respond differently and no longer precisely cancel at the summer. As this innovation,  $(\hat{y} - y)$  propagates through the embedded classical controller; the gain  $G_c$  offers an extra degree of freedom to improve the system robustness. In effect, the control input is modified to compensate for plant modeling uncertainties.

## V. AN INITIAL DEMONSTRATION OF SFAC ROBUSTNESS

To demonstrate the robustness advantage of the SFAC configuration, a specific uncertainty between plant and observer needs to be considered. The first thing that a robust controller based on one-delayed neutron group must be capable of is control of a much higher order process with many delayed neutron groups. By considering a six-delayed neutron group representation, the plant  $\mathbf{A}$  matrix of Eqs. (9) and (10) becomes

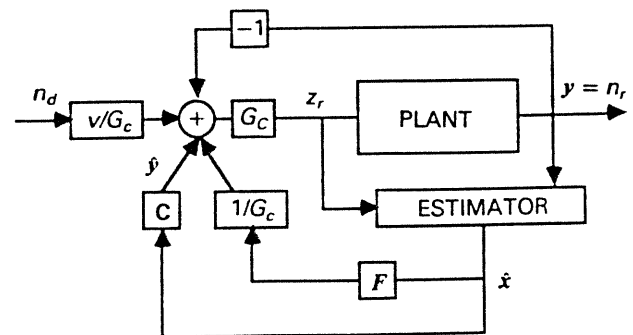


Fig. 5. Introduction of an embedded classical controller in a CSFC for derivation of the SFAC gain vector  $F_m$  from the CSFC gain vector  $F$ .

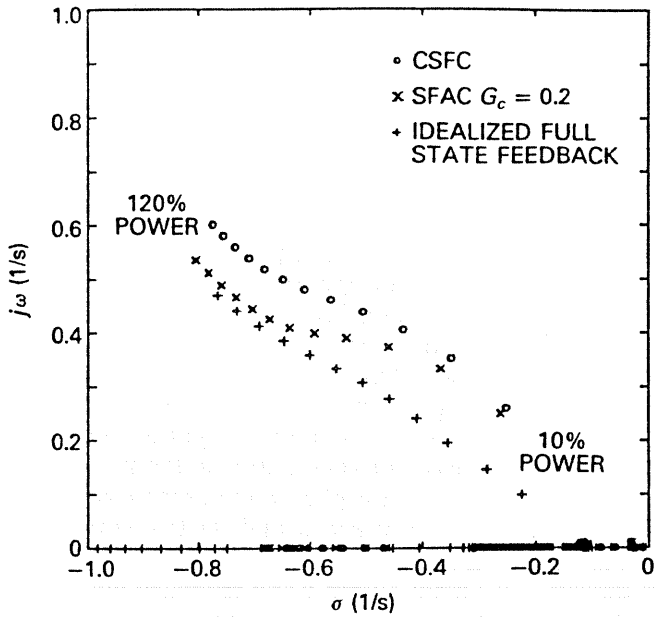


Fig. 6. Dominant eigenvalue sensitivity of SFAC and CSFC one-delayed neutron group model-based observer state feedback controllers for application to a six-delayed neutron group plant.

tenth order while the observer  $A_o$  matrix remains at fifth order. To better estimate the reactor states, the nonlinear reactor kinetics equations are used in the observer, which causes the observer  $A_o$  matrix to have the same variation because of the equilibrium relative power level parameter  $n_{r0}$  as the plant  $A$  matrix. The sensitivity of the dominant eigenvalue of the CSFC and SFAC configurations is shown in Fig. 6. The six-delayed neutron group parameters are summarized in Table II.

The first thing to note in Fig. 6 is that the idealized full state feedback dominant eigenvalue behavior as

TABLE II

Effective Six-Delayed Neutron Group Parameters at the Middle of the Cycle of a TMI-Type PWR\*

Group $i$	$\beta_i$	$\lambda_i$ ( $s^{-1}$ )
1	0.000215	0.0124
2	0.001424	0.0305
3	0.001274	0.111
4	0.002568	0.301
5	0.000748	1.14
6	0.000273	3.01

\*See Ref. 12.

power level is varied from 120 to 10% is naturally different than in Fig. 3 because of the difference in the order of the idealized models; Fig. 3 is a fifth-order plant; Fig. 6 is a tenth-order plant. Both optimal controller designs used the same performance index [Eq. (5)] for calculating the required gains. The second thing to note in Fig. 6 is that the low-order CSFC configuration slightly shifts the dominant eigenvalue to the less stable region at all power levels. The third and most important thing to note is that the SFAC configuration demonstrates a less severe shift in dominant eigenvalue than the CSFC configuration at all power levels. Figure 7 further assesses the tunable robustness characteristic of the SFAC configuration for classical control gains of 0.001, 0.1, 0.3, and 0.5. As the classical control gain approaches zero, the SFAC dominant eigenvalue behavior approaches that of the CSFC configuration. As  $G_c$  is increased, the dominant eigenvalue becomes more damped. However, the embedded classical control gain cannot simply be made arbitrarily large because observer poles at  $\sigma = -2.34$  and  $\sigma = -1.52$  for the design condition, Table I and Eq. (7), become overly sensitive as controller gain  $G_c$  is increased. Figure 8 (with a change in scale) demonstrates the sensitivity of the feedback and observer poles at embedded classical controller gains of 0.75, 1.5, 3.0, and 6.0. The embedded classical control gain is recommended to be set based on classical output feedback analysis such as root locus. For the foregoing reactor control problem, root locus analysis suggests a classical control gain of  $G_c = 0.2$ .

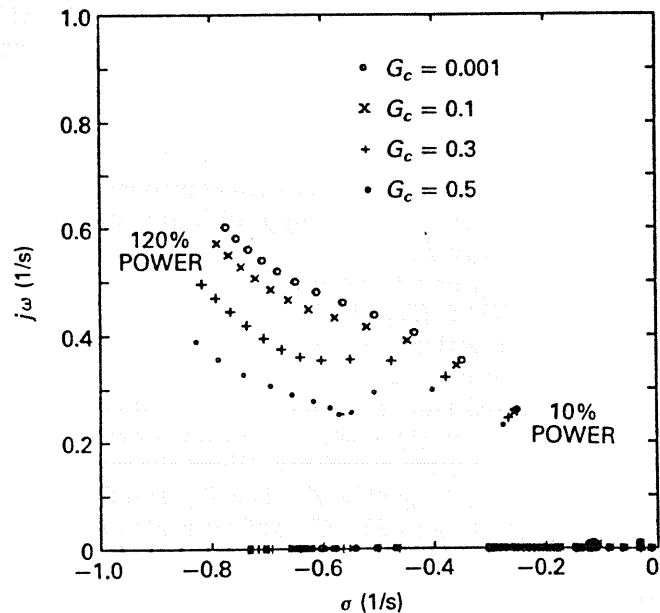


Fig. 7. SFAC dominant eigenvalue sensitivity for power levels in the range of 10 to 120% and embedded classical controller gains of 0.001, 0.1, 0.3, and 0.5.



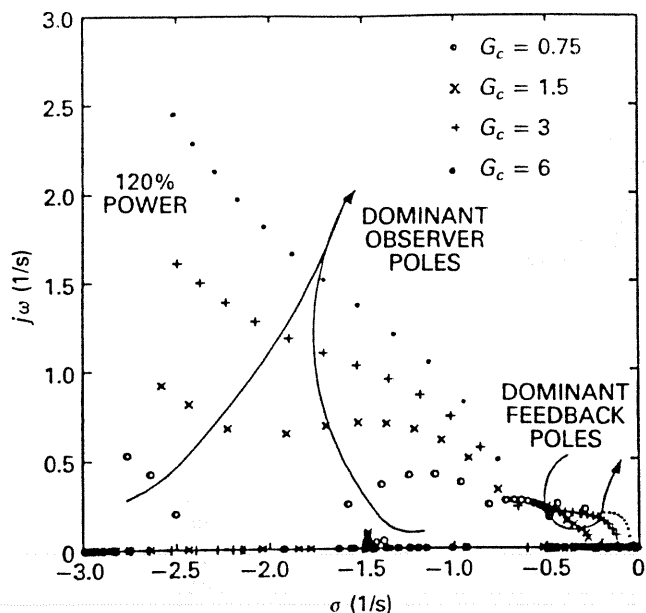


Fig. 8. SFAC dominant eigenvalue sensitivity for power levels in the range of 10 to 120% and embedded classical controller gains of 0.75, 1.5, 3, and 6.

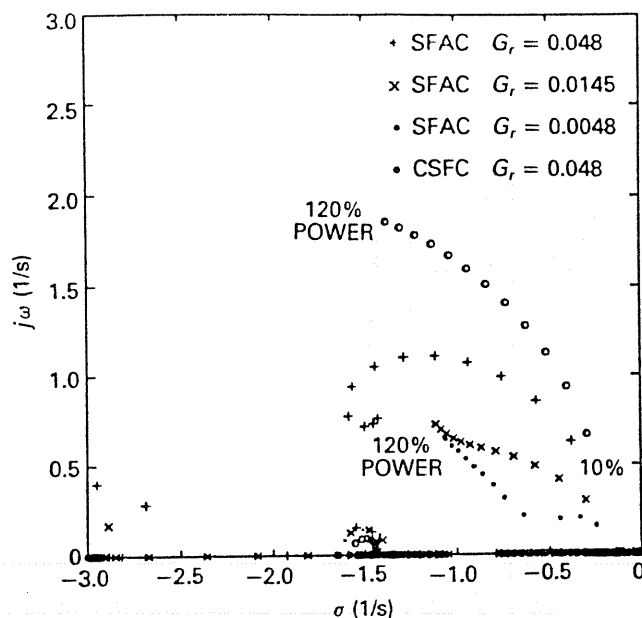


Fig. 9. SFAC dominant eigenvalue sensitivity for power levels from 120 to 10% and control rod worths of 0.0048, 0.0145 (design), and 0.048.

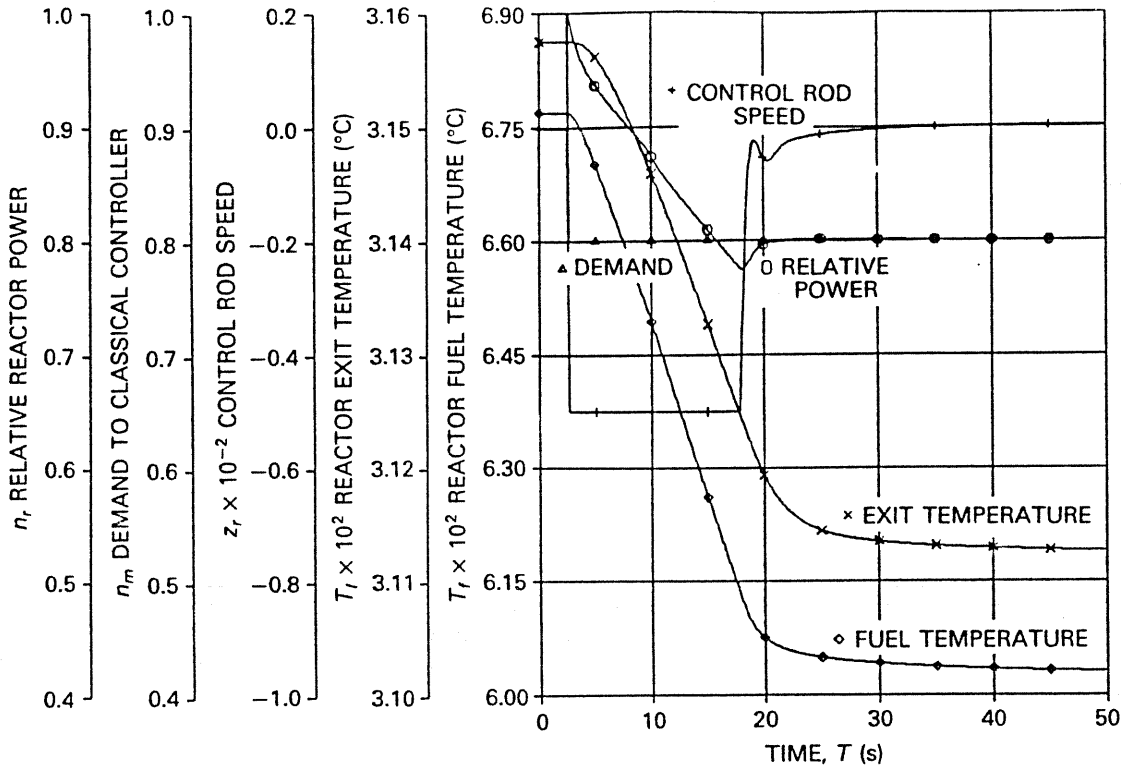
## VI. THE EFFICACY OF THE SFAC ROBUSTNESS CHARACTERISTIC

Another known source of uncertainties that a robust reactor power controller must accommodate is that most of the other plant parameters change as a result of normal fuel burnup, power level, and/or control rod position. To meet the strict definition of a robust controller as time invariant, the robust controller uses constant values for all parameters. Although gain scheduling, adaptive identification, adaptive control, and nonlinear control offer approaches to compensate for plant parameter variations, a time-invariant controller that achieves desired performance, stability, and fault accommodation is preferable because of its much simpler implementation requirements. To further assess the potential for a robust fifth-order controller based on one-delayed neutron group, the Babcock & Wilcox (B&W) modular modeling system (MMS) model of a TMI-type PWR was used.<sup>12</sup> The MMS model is a twenty-third-order nonlinear simulation that models the reactor with three axial thermal-hydraulic and associated reactor kinetics calculations. Three-delayed neutron groups are represented at each axial node, and the prompt jump approximation is used. Parameter variations due to fuel burnup, power level, and control rod position are modeled. A parameter with a large variation and concern is the control rod worth  $G_r$ . Figure 9 shows the SFAC dominant eigenvalue sensitivity analysis ( $G_c = 0.2$ ) for the 10 to 120% power range with three different values of plant con-

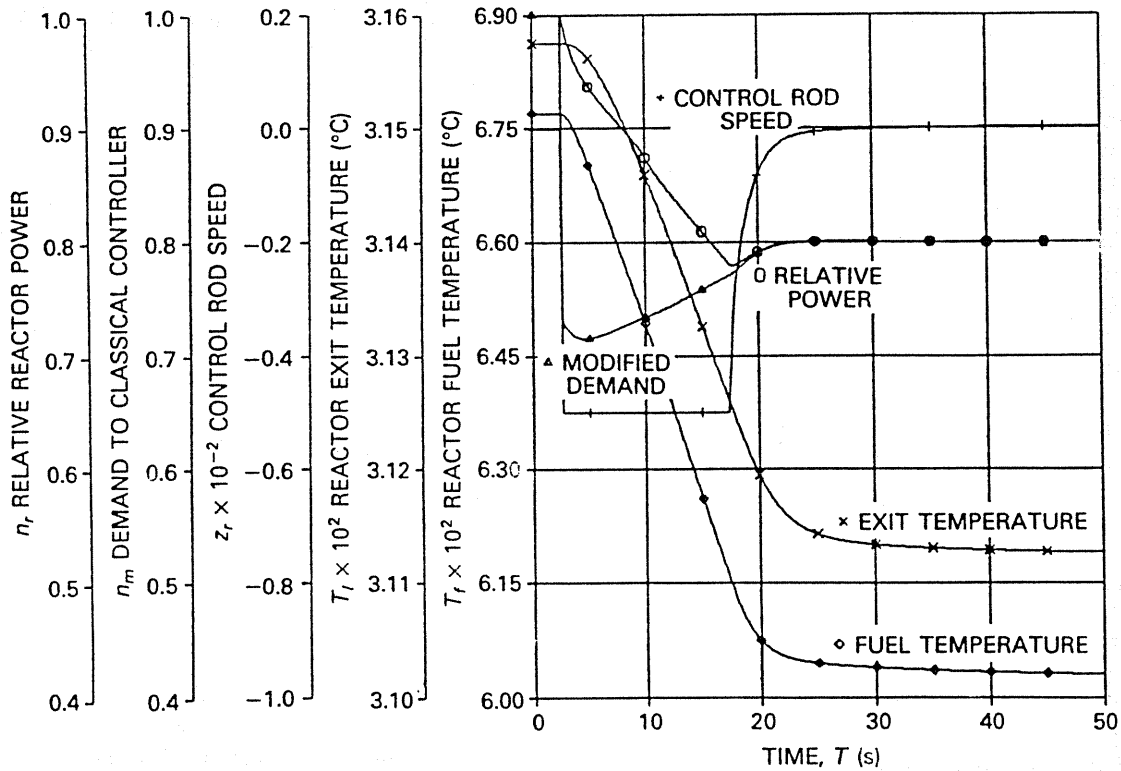
trol rod group worth:  $G_r = 0.0048$ ,  $G_r = 0.0145$  (nominal value from Table I), and  $G_r = 0.048$ . The CSFC dominant eigenvalue sensitivity with the high-worth rod group is also shown as a lower bound for the damping ratio characteristic of the SFAC configuration. For the case of the high-worth rod group, the CSFC dominant eigenvalue indicates a noticeably poorer damping ratio. The linear analysis prediction (Fig. 9) is confirmed for a step change in demand transient from 100 to 80% power using the nonlinear MMS (Fig. 10). The CSFC response (Fig. 10a) shows a lightly damped control rod group speed, whereas the SFAC response (Fig. 10b) shows a noticeably better damping characteristic when the control element becomes unsaturated at a maximum speed of 0.005 fraction of core length/s. Results of numerous dominant eigenvalue sensitivity analyses and simulations that confirm the robustness advantage of the SFAC configuration over the power range of 10 to 100% and over the full range of burnup conditions are presented in Ref. 4.

## VII. SUMMARY AND CONCLUSION

The robustness advantage of implementing model-based controllers with an embedded classical controller has been demonstrated for a fifth-order robust reactor power controller design for a TMI-type PWR. The demonstration utilized a dominant eigenvalue sensitivity analysis based on a linearized model of a simulated plant and controller. The improvement in robustness



(a)



(b)

Fig. 10. Verification of the SFAC robustness characteristic using nonlinear simulation: (a) CSFC response with a high worth rod for a step change in demand from 100 to 80% and (b) SFAC response.

of the SFAC relative to a CSFC configuration was first demonstrated with the sensitivity analysis procedure by considering the specific discrepancy of a six-delayed neutron group reactor simulation controlled by a one-delayed neutron group controller. The linear analysis robustness predictions were further confirmed via application of the fifth-order controller to a much higher order nonlinear reactor simulation using the B&W MMS (Ref. 12). The efficacy of the SFAC configuration for significantly improving the robustness of a model-based controller implementation was then demonstrated for an extreme case of severe parameter uncertainty; the control rod reactivity worth of the plant was varied by a factor of 3, while the controller model's rod worth parameter remained constant at the nominal design value.

The conventional feedback controller embedded within a state feedback system is a multiple layer controller that achieves improved robustness characteristics of modern control implementations for power plant applications. Coupled with the previous motivation<sup>1</sup> to provide an intuitive interpretation of the operation of an optimal control design, the SFAC concept appears to be a potentially powerful vehicle for improving wide-range operation of power plants. This multiple controller technique can also provide improved fault-accommodating characteristics in power plant control.<sup>13</sup>

#### ACKNOWLEDGMENT

This work was supported in part by a grant from the U.S. Department of Energy (DOE), DE-FG07-89ER12889. However, any findings, conclusions, or recommendations expressed herein are those of the authors and do not necessarily reflect the views of the DOE.

#### REFERENCES

1. R. M. EDWARDS, K. Y. LEE, and M. A. SCHULTZ, "State Feedback Assisted Classical Control: An Incremental Approach to Control Modernization of Existing and Future Nuclear Reactors and Power Plants," *Nucl. Technol.*, **92**, 167 (1990).
2. J. LUNZE, *Robust Multivariable Feedback Control*, Prentice-Hall International, Hemphstead, U.K. (1988).
3. H. E. GARCIA, A. RAY, and R. M. EDWARDS, "Reconfigurable Control of Power Plants Using Learning Automata," *IEEE Control Systems Mag.*, **11**, 1, 85 (1991).
4. R. M. EDWARDS, "Robust Optimal Control of Nuclear Reactors," PhD Thesis, The Pennsylvania State University (May 1991).
5. D. E. KIRK, *Optimal Control Theory, An Introduction*, Prentice-Hall, Englewood Cliffs, New Jersey (1970).
6. M. A. SCHULTZ, *Control of Nuclear Reactors and Power Plants*, 2nd ed., McGraw-Hill, New York (1961).
7. C. T. CHEN, *Linear Systems Theory*, Holt, Rinehart, and Winston, New York (1984).
8. ANALYTICAL SCIENCES CORPORATION, *Applied Optimal Estimation*, A. GELB, Ed., MIT Press, Cambridge, Massachusetts (1974).
9. G. STEIN and M. ATHANS, "The LQG/LTR Procedure for Multivariable Feedback Control Design," *IEEE Trans. Automatic Control*, **AC-32**, 2, 105 (1987).
10. G. V. MURPHY and J. M. BAILEY, "Robust Control Technique for Nuclear Plants," ORNL/TM-10916, Oak Ridge National Laboratory (Mar. 1989).
11. D. C. YOULA, J. J. BONGIORNO, Jr., and C. N. LU, "Single Loop Feedback-Stabilization of Linear Multivariable Dynamical Plants," *Automatica*, **10** (1974).
12. BABCOCK AND WILCOX COMPANY, "Modular Modeling System (MMS): A Code for Dynamic Simulation of Fossil and Nuclear Power Plants—Overview and General Theory," CS/NP-2989, Electric Power Research Institute (Mar. 1983).
13. R. I. REYES, D. R. MUDGETT, and K. Y. LEE, "Power System Stabilization via Additive Multiple Adaptive Controller," *Proc. 29th Conf. Decision and Control*, Honolulu, Hawaii, December 1990, p. 3077.

---

**Robert M. Edwards** (BS, nuclear engineering, The Pennsylvania State University (PSU), 1971; MS, nuclear engineering, University of Wisconsin, 1972; PhD, nuclear engineering, PSU, 1991) is an assistant professor of nuclear engineering at PSU. He has been conducting research in real-time diagnostics and advanced control at PSU since 1987 and teaches courses in reactor control and reactor experiments. Prior experience includes transient thermal-hydraulic code development and control systems analysis of large high-temperature gas-cooled reactors.

**Kwang Y. Lee** (PhD, system science, Michigan State University, 1971) is an associate professor of electrical engineering at PSU. His areas of interest

are optimal control, system identification, robust control, and artificial intelligence, and their applications to large-scale systems and power systems.

**Asok Ray** (PhD, mechanical engineering, Northeastern University, Boston, 1976) is a professor of mechanical engineering at PSU. His research experience and interests include control and optimization of continuously varying and discrete-event dynamic systems in both deterministic and stochastic settings, intelligent instrumentation for real-time distributed processes, and design of fault-accommodating robust control systems.